ORNL/TM-2016/252
Revision: 0

Survey of Thermal-Fluids Evaluation and Confirmatory Experimental Validation Requirements of Accident Tolerant Cladding Concepts with Focus on Boiling Heat Transfer Characteristics

Fuel Cycle Research & Development Advanced Fuels Campaign

N. R. Brown, A. J. Wysocki, K. A. Terrani
Oak Ridge National Laboratory

A. Ali, M. Liu, E. Blandford
University of New Mexico

Prepared for
U. S. Department of Energy
Office of Nuclear Energy

June 2016
M3FT-16OR020204032

ORNL/TM-2016/252
Revision 0

Survey of Thermal-Fluids Evaluation and Confirmatory Experimental Validation Requirements of Accident Tolerant Cladding Concepts with Focus on Boiling Heat Transfer Characteristics

N. R. Brown, A. J. Wysocki, K. A. Terrani
Oak Ridge National Laboratory

A. Ali, M. Liu, E. Blandford
University of New Mexico

June 2016

Prepared by
OAK RIDGE NATIONAL LABORATORY
Oak Ridge, TN 37831-6283
managed by
UT-BATTELLE, LLC
for the
US DEPARTMENT OF ENERGY
under contract DE-AC05-00OR22725

INTENTIONALLY BLANK

ABSTRACT

The U.S. Department of Energy Office of Nuclear Energy (DOE-NE) Advanced Fuels Campaign (AFC) is working closely with the nuclear industry to develop fuel and cladding candidates with potentially enhanced accident tolerance, also known as accident tolerant fuel (ATF). Thermal-fluids characteristics are a vital element of a holistic engineering evaluation of ATF concepts. One vital characteristic related to boiling heat transfer is the critical heat flux (CHF). CHF plays a vital role in determining safety margins during normal operation and also in the progression of potential transient or accident scenarios.

This deliverable is a scoping survey of thermal-fluids evaluation and confirmatory experimental validation requirements of accident tolerant cladding concepts with a focus on boiling heat transfer characteristics. The key takeaway messages of this report are:

1. CHF prediction accuracy is important and the correlations may have significant uncertainty.

2. Surface conditions are important factors for CHF, primarily the wettability that is characterized by contact angle. Smaller contact angle indicates greater wettability, which increases the CHF. Surface roughness also impacts wettability. Results in the literature for pool boiling experiments indicate changes in CHF by up to 60% for several ATF cladding candidates.

3. The measured wettability of FeCrAl (i.e., contact angle and roughness) indicates that CHF should be investigated further through pool boiling and flow boiling experiments.

4. Initial measurements of static advancing contact angle and surface roughness indicate that FeCrAl is expected to have a higher CHF than Zircaloy. The measured contact angle of different FeCrAl alloy samples depends on oxide layer thickness and composition. The static advancing contact angle tends to decrease as the oxide layer thickness increases.

INTENTIONALLY BLANK

CONTENTS

FIGURES

TABLES

ACRONYMS

ASTM	American Society of Testing Materials
ATF	Accident Tolerant Fuel
ATR	Advanced Test Reactor
ATWS	Anticipated Transient Without SCRAM
BWR	Boiling Water Reactor
CHF	Critical Heat Flux
DNB	Departure from Nucleate Boiling
DNBR	Departure from Nucleate Boiling Ratio
DOE	Department of Energy
FeCrAl	Iron-Chromium-Aluminum Alloy
INL	Idaho National Laboratory
ORNL	Oak Ridge National Laboratory
PWR	Pressurized Water Reactor
RIA	Reactivity Initiated Accident
SiC	Silicon Carbide
TREAT	Transient Reactor Test Facility

ACKNOWLEDGEMENTS

This work was supported by the US Department of Energy Office of Nuclear Energy (DOE-NE) Advanced Fuels Campaign. The authors greatly appreciate the thoughtful reviews of M. Scott Greenwood and Kevin Robb at Oak Ridge National Laboratory.

Survey of Thermal-Fluids Evaluation and Confirmatory Experimental Validation Requirements of Accident Tolerant Cladding Concepts with Focus on Boiling Heat Transfer Characteristics

1. INTRODUCTION

The U.S. Department of Energy Office of Nuclear Energy (DOE-NE) Advanced Fuels Campaign (AFC) is working closely with the nuclear industry to develop fuel and cladding candidates with potentially enhanced accident tolerance, also known as accident tolerant fuel (ATF). One over-arching objective of the AFC is a lead fuel assembly or lead fuel rod irradiation in a commercial nuclear power reactor by 2022 [1]. The AFC is considering a variety of potential candidate fuel and cladding materials. One promising candidate for a cladding material with potentially enhanced accident tolerance is the iron-chromium-aluminum alloy known as FeCrAl. The FeCrAl alloys feature significantly enhanced oxidation resistance versus the present reference Zr-based alloys utilized in state-of-the-art light water reactors (LWRs) [2]. Among others, General Electric Global Research proposes FeCrAl alloys as potentially accident tolerant cladding materials [3].

The AFC is conducting four experimental testing series prior lead fuel assembly or lead fuel rod irradiation in a commercial nuclear power reactor [1]. These include irradiation tests (referred to as ATF-1) at the Advanced Test Reactor (ATR) at Idaho National Laboratory (INL), PWR prototypical loop tests (referred to as ATF-2) also at ATR, and transient testing at the Transient Reactor Test Facility (TREAT) at INL (referred to as ATF-3 and ATF-4). In addition, tests are planned in the Halden reactor in Norway and also in the commercial nuclear power reactor where the lead fuel assembly or lead fuel rod irradiation will be conducted. A list of planned testing is reviewed in Reference 1 and 4.

Technology implementation of potentially enhanced accident tolerant cladding requires understanding of not only the characteristics of the material and performance during normal operation, but also behavior during transient events or accidents [5]. This encompasses reactor performance and safety characteristics [6] as well as a wide variety of materials behavior and engineering issues, including high temperature environment behavior, oxidation environment behavior, irradiation behavior, fuel cladding mechanical interaction, and cladding degradation and failure mechanisms, among many other issues [5].

In addition to the issues identified above, thermal-fluids characteristics are a vital element of a holistic engineering evaluation of ATF concepts [5]. Proposed fuel and cladding candidates may have different thermal-fluids performance from the reference zirconium-based cladding material. In particular, the boiling heat transfer characteristics of these concepts as well as overall core pressure drop may be affected by clad selections with differing microstructures and surface characteristics.

One significant quantity related to safety limits in both pressurized water reactors (PWRs) and boiling water reactors (BWRs) is the critical heat flux (CHF). At CHF, the efficacy of heat transfer rapidly degrades and components can heat up rapidly. CHF is the heat flux at which the departure from nucleate boiling (DNB) occurs in PWRs. DNB is directly relevant to the departure from nuclear boiling ratio (DNBR), which is the ratio between the critical heat flux and the actual heat flux. Surface wettability is an important factor that influences CHF [7, 8].

CHF is a vital parameter for technology implementation of FeCrAl as an accident tolerant cladding material [5]. Significant changes in CHF properties and boiling heat transfer characteristics will

impact the progression of transient and accident events and reactor safety characteristics. Additionally, the behavior of the candidate cladding materials post-CHF impacts reactor safety.

This report is focused on a scoping assessment of the impact of CHF characteristics of ATF cladding and a general overview of the importance of changes in CHF on thermal fluid and reactor safety characteristics. The report illustrates why boiling heat transfer characteristics are important, reviews factors that can impact CHF characteristics and recent efforts in the literature relevant to ATF, and documents some recent experimental results that enhance understanding of how one candidate ATF cladding (FeCrAl) might impact CHF. The specific contents and focus areas of this deliverable are:

(1) Scoping parametric analyses using thermal hydraulic sub-channel and systems analysis codes to illustrate the importance of boiling heat transfer characteristics, and in particular changes in CHF, in the progression of some transient and/or accident events,

(2) Review of a few selected recent efforts focused on CHF from the literature that are relevant to ATF, and

(3) Experimental results from measurement of static advancing contact angle for FeCrAl, Zircaloy, and Stainless Steel samples that have been exposed to PWR and BWR relevant environments.

2. SCOPING PARAMETRIC ANALYSES TO SHOW THE IMPACT OF CHF CHARACTERISTICS ON ACCIDENT PROGRESSION

The objective of this section is to illustrate the potential importance of changes in boiling heat transfer characteristics, and specifically CHF, on the progression of some accidents in both PWRs and BWRs. The parametric evaluations in this report are not intended to be representative of any particular ATF cladding concept or the specific impact on boiling heat transfer that a particular concept might have. Rather, these studies are focused on illustrating the potential importance of CHF and the impact on a vital safety parameter, namely the peak cladding temperature.

Changes in CHF will have an impact on safety margins during normal operating conditions and transient or accident conditions. In normal operation, a change in CHF will change the safety margin by impacting the DNBR in PWRs or Minimum Critical Power Ratio (MCPR) in BWRs and may make a particular operating condition that is acceptable for one cladding material be unacceptable for another cladding material.

The potential impacts of a change in CHF were explored via analysis of a rapid power ramp transient in a PWR, representative of a super-prompt reactivity initiated accident (RIA). In addition, the impact of CHF on a BWR anticipated transient without SCRAM (ATWS) were analyzed.

2.1 PWR RIA TRANSIENT EXAMPLE

There are two phases to a super-prompt RIA [9]. The first phase is the low temperature phase dominated by pellet-cladding interaction, where the energy released in the RIA is deposited nearly adiabatically in the fuel. The fuel mechanically interacts with the cladding in this phase. The second phase is the high temperature phase, where the energy is transferred to the coolant, which may cause DNB in a PWR. This analysis is focused on the DNB phase, and in particular the impact of changes in CHF on the phase of the transient where the energy deposited is transferred to the coolant. The impact of RIA was studied via a power ramp transient using the COBRA-EN subchannel code [10]. A generic radial power distribution from an example model [10] was assumed with one channel per assembly. The assumed parameters for the reactor model are shown in Table 1.

Table 1. Model parameters for rapid power ramp transient.

Parameter	Value
Reactor core heat output, MW(th)	2988
System pressure, nominal, MPa	14.91
Inlet coolant temperature, ^{o}C	292.9
Fuel assembly design	17×17
Active fuel height, cm	426.7
Number of fuel assemblies	157
Fuel assembly pitch, cm	21.5
Channels per assembly	1 (Average channel)
Channels in model	26 (1/8th core)

The calculations are thermal hydraulic and do not include any neutronic feedback. It is notable that the thermal hydraulic models in COBRA-EN are not optimal for predicting two-phase flow behavior in transients for post-CHF conditions. COBRA-EN contains several homogeneous three- and four-equation models that are more accurate for pre-CHF conditions. In addition, the COBRA-EN manual states: *"the numerical behavior of the relevant [post-CHF] correlations has not been fully tested."* CHF correlations have a set uncertainty for a narrow range of conditions and this uncertainty impacts safety margins. These scoping calculations illustrate the importance of narrowing the uncertainty of CHF prediction with experimental measurements. The generic power ramp assumed in the modeling is shown in Fig. 1.

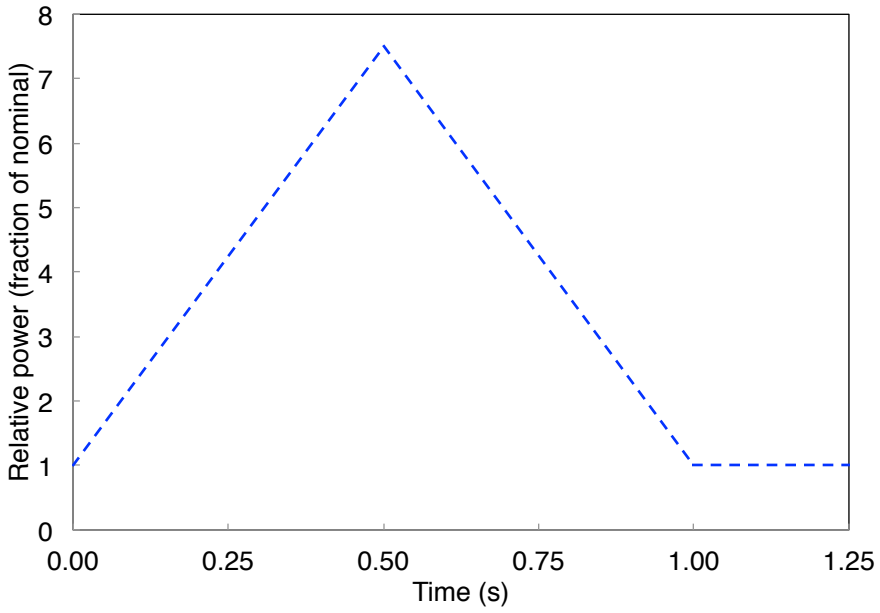

Fig. 1. Rapid power ramp transient boundary condition.

In these calculations a constant multiplier of 0.75 or 1.25 is used to perturb the Electric Power Research Institute (EPRI) CHF correlation [11] used by COBRA-EN. The objective of this multiplier is to illustrate the potential impacts of these changes in CHF on the transient. These scoping parametric calculations are not representative of any particular concept or a realistic transient. Fig. 2 shows the variation of minimum DNBR at a given axial location during the transient for the constant multipliers of

0.75 or 1.25 and the base case with a multiplier of unity. This example illustrates how the reduction in CHF for the case with a 0.75 multiplier yields a DNBR of below 1.0 during the transient. The poor heat transfer yields very high cladding temperatures, as shown in Fig. 3 and increased fuel temperatures as shown in Fig. 4.

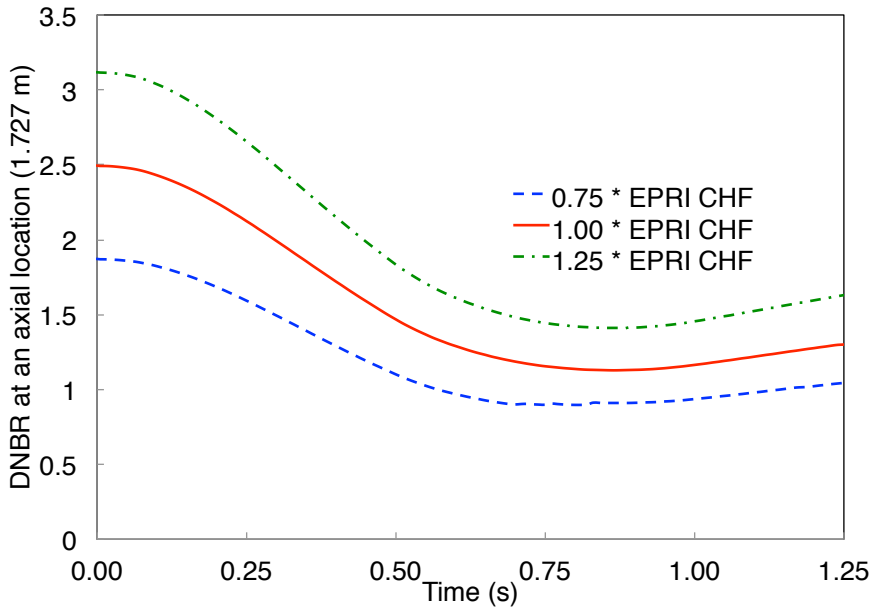

Fig. 2. Minimum DNBR during the power ramp transient with the EPRI CHF correlation using constant multipliers of 0.75, 1.00, and 1.25.

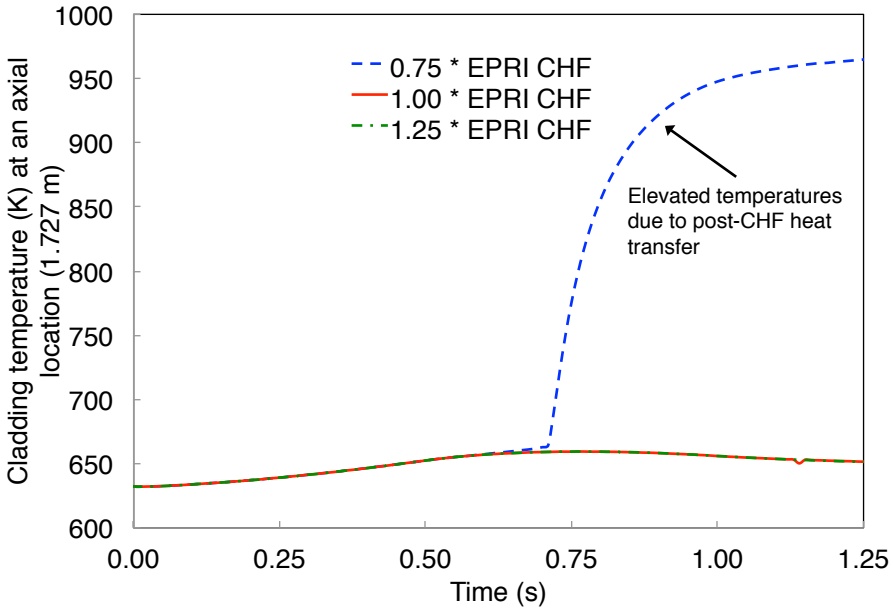

Fig. 3. Peak cladding temperature during the power ramp transient.

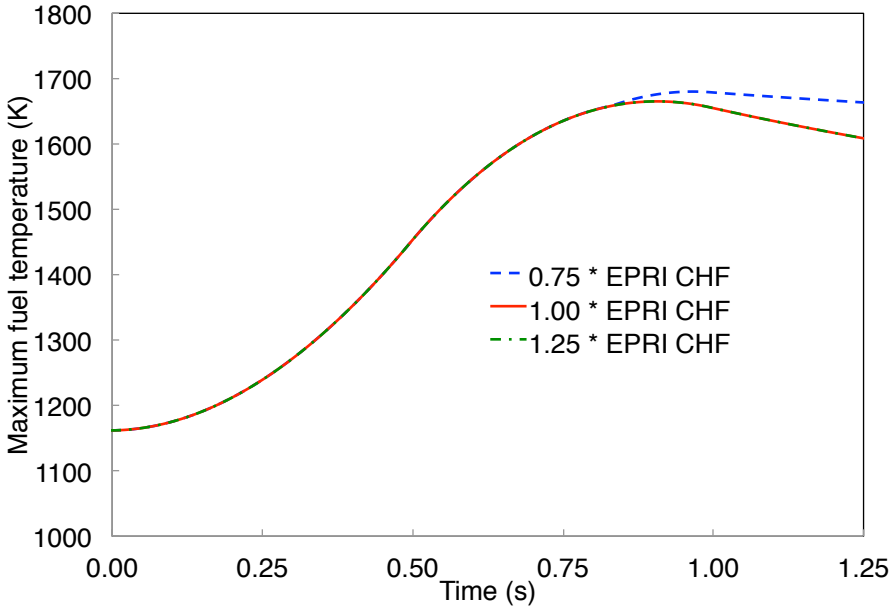

Fig. 4. Maximum fuel temperature during the power ramp transient.

The impact of the post-CHF behavior on the hot channel heat flux is shown in Fig. 5 as a function of the axial height of the channel at a state-point 1.0 seconds into the transient. Similarly, the impact on the cladding temperature in the hot channel is shown in Fig. 6.

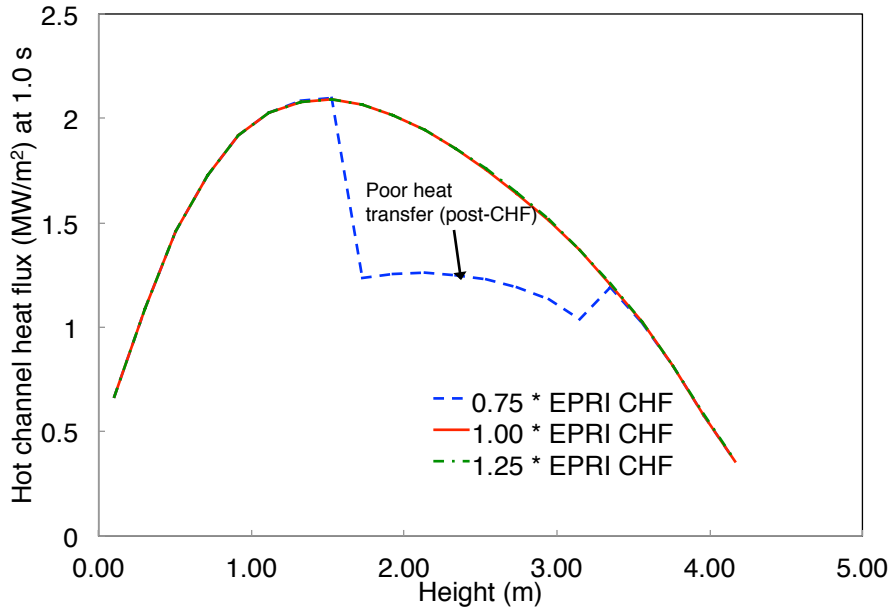

Fig. 5. Axial heat flux distribution at t=1.0 s, the degraded heat transfer is due to post-DNB behavior.

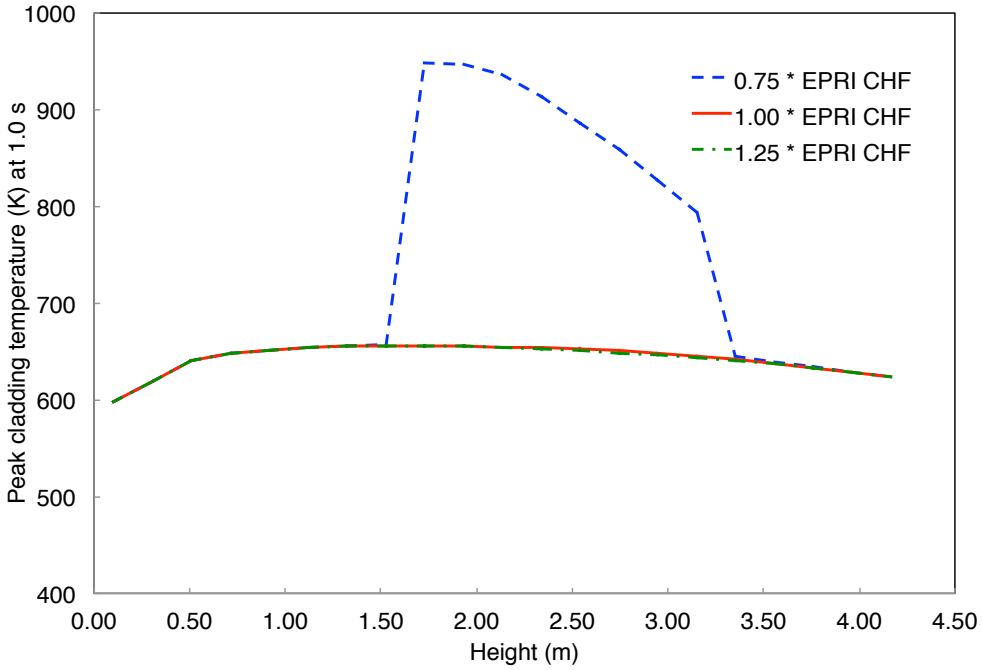

Fig. 6. Axial cladding temperature distribution at t=1.0 s, degraded heat transfer is due to post-DNB behavior.

The response to this contrived transient illustrates the potential sensitivity to changes in the CHF value. These changes will impact safety margins and may significantly impact the progression of a transient or accident scenario.

2.2 BWR ATWS TRANSIENT EXAMPLE

A hypothetical BWR ATWS-I (ATWS with instability) event was simulated using the U.S. NRC coupled 3D neutronic/thermal-hydraulic code system TRACE/PARCS [12, 13]. The TRACE/PARCS code has been successful in reproducing real-world ATWS-I event behavior in previous studies, such as the OECD Oskarshamn-II stability benchmark [14] and the OECD Ringhals stability benchmark [15]. The current analysis relies on a simplified version of the Ringhals model, with uniform fuel loading and quarter-core symmetry boundary conditions. Unlike in a previous study which used a similar model [16], the use of symmetry boundary conditions in the current study precluded out-of-phase oscillations, in favor of in-phase oscillations, to achieve the simplest and clearest results for the purposes of this basic scoping study. The second-order spatial discretization method was selected in TRACE to avoid the significant artificial damping effect seen in previous BWR stability calculations [15, 17].

The most common type of instability in commercial BWRs is the coupled neutronic-thermohydraulic instability, which can be understood as density-wave oscillations coupled to the neutron kinetics via temperature and moderator density feedback [18]. This class of instability can develop under low flow and relatively high power conditions; this so-called “exclusion region” of the power-flow operating map is therefore avoided during normal operating conditions and reactor startup. However, certain types of ATWS can bring the core into this unstable region, particularly when starting from Maximum Extended Load Line Limit Analysis Plus (MELLLA+) conditions [19].

In the present study, a recirculation pump rundown from 90 revolutions per minute (RPM) to 35 RPM was used to bring the simulated BWR core from stable steady-state operating conditions into ATWS-like conditions at low flow rate and relatively high power, creating unstable conditions in which

in-phase oscillations grew over time. In some cases, the simulation reached a user-defined simulation end time of 300 seconds; in other cases, the code aborted prior to the requested end time of 300 seconds due either to numerical convergence issues or exceeding the cladding (or fuel) melting temperatures.

To examine the possible significance of wettability on the ATWS-I progression, two separate studies were performed: one which varied the CHF values calculated by TRACE, and one which varied the minimum stable film boiling temperature (T_{min}) values calculated by TRACE.

In the first study, CHF values calculated by TRACE, using the AECL-IPPE CHF lookup tables, were adjusted using the formula:

$$q''_{CHF} = K_{CHF} \cdot q''_{CHF,0}\,, \tag{1}$$

where $q''_{CHF,0}$ is the original critical heat flux value calculated by TRACE (calculated uniquely for each timestep and spatial node in the core), K_{CHF} is a multiplier, and q''_{CHF} is the final CHF value used by TRACE for the given timestep and spatial node.

Fig. 7 and Fig. 8 give the results for core power and peak clad temperature (PCT) for three different values of K_{CHF}. In each case, the oscillations grew in magnitude until the CHF was exceeded in one or more channels. For the case of $K_{CHF} = 0.5$, this resulted immediately in a runaway increase in PCT due to the poor heat transfer characteristics of the cladding surface. The calculation terminated due to the cladding melting temperature being exceeded around 200 s.

A unique feature of the BWR stability phenomenon is the possibility of rapid, repeated cycling between dryout and rewet conditions due to the large periodic swings in power and flow rate over a very short time period (roughly 2.5 seconds between successive power peaks). This behavior was observed for the case of $K_{CHF} = 1.0$ for roughly 20 seconds (8 oscillation periods) and for $K_{CHF} = 1.5$ for roughly 25 seconds (10 oscillation periods). Cyclic rewet was possible in these cases but not for the $K_{CHF} = 0.5$ case because (1) fewer numerical nodes experienced dryout, allowing the cladding surface temperature to return below T_{min} more quickly due to axial heat conduction from neighboring nodes, and (2) the threshold for re-initiating dryout after rewet was higher.

In each case, the oscillations eventually grew large enough in magnitude to cause runaway PCT increase (up to the equilibrium PCT value dictated by the steam heat transfer coefficient) due to total failure to rewet; however, this study demonstrates that a cladding material with better wettability characteristics (in terms of CHF) may increase the time before clad melting or other severe consequences during an ATWS-I event.

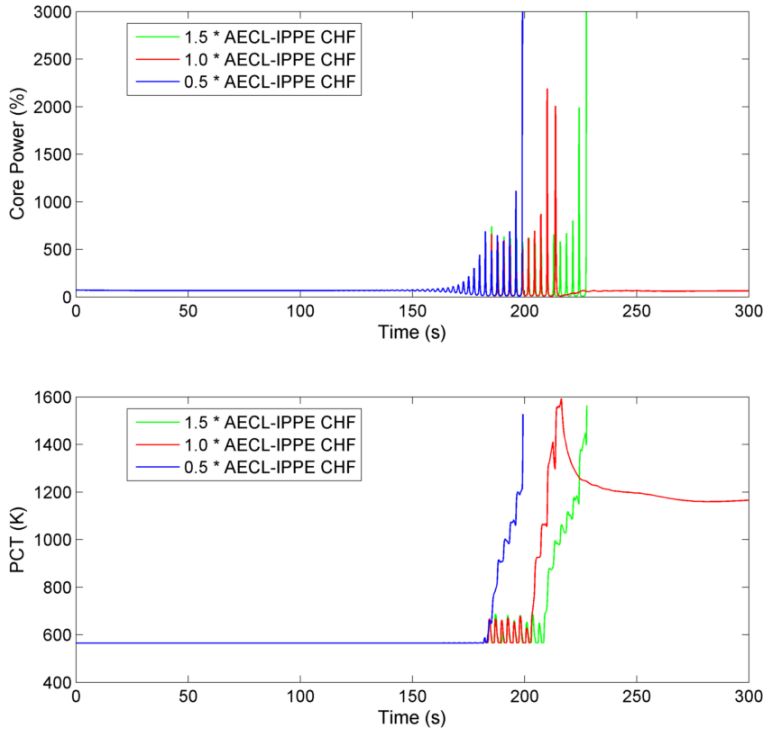

Fig. 7 - Core power (top) and peak clad temperature (PCT) (bottom) during the hypothetical ATWS-I event, using three different multipliers to adjust the internally-calculated CHF values

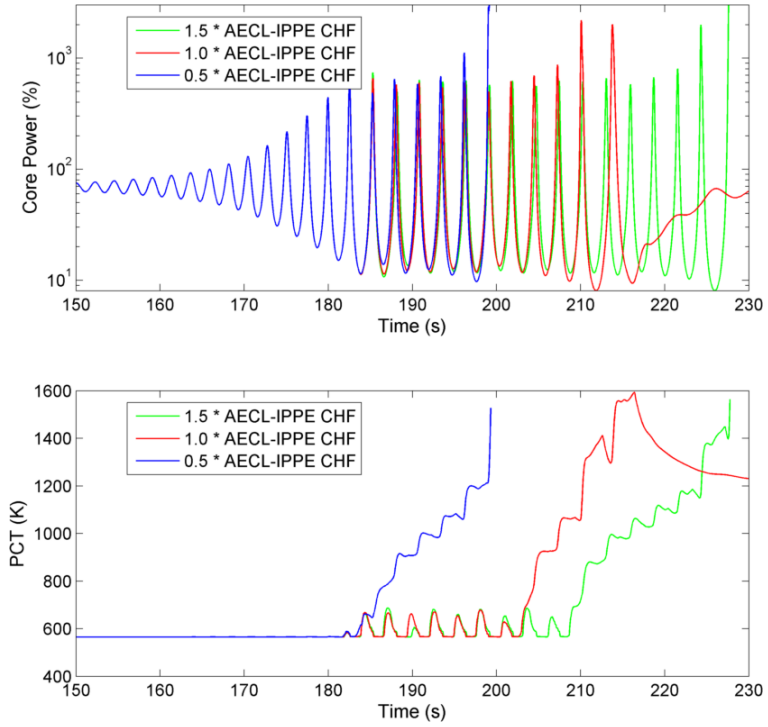

Fig. 8 - Close-up of core power (top) and PCT (bottom) for the CHF study

In the second study, the default CHF values calculated by TRACE were used, but T_{min} values calculated by TRACE (which uses the Groeneveld-Stewart model) were adjusted using the formula:

$$T_{min} = T_{sat} + K_{T_{min}}\left(T_{min,0} - T_{sat}\right), \quad (2)$$

where $T_{min,0}$ is the original minimum stable film boiling temperature calculated by TRACE (calculated uniquely for each timestep and spatial node in the core), T_{sat} is the saturation temperature for the given timestep and spatial node, $K_{T_{min}}$ is a multiplier, and T_{min} is the final value used by TRACE for the given timestep and spatial node. This multiplier was applied by modifying the TRACE source code directly.

Fig. 9 and Fig. 10 show the core power and PCT results for three different $K_{T_{min}}$ values. As before, the base case ($K_{T_{min}} = 1.0$) gave cyclic dryout and rewet for roughly 20 seconds until steady dryout occurred, causing a several hundred degree Celsius spike in PCT. For the $K_{T_{min}} = 1.5$ case, the cyclic dryout and rewet occurred over roughly a 45 second span until steady dryout occurred. However, for the $K_{T_{min}} = 2.0$, the cyclic dryout and rewet continued indefinitely, or at least through the final 120 seconds until the specified simulation end time of 300 seconds was reached. Increasing the T_{min} values lowered the cladding temperature threshold at which rewet could occur, allowing the cladding temperature to remain within roughly 150° C of the cladding temperatures at normal steady-state operating conditions.

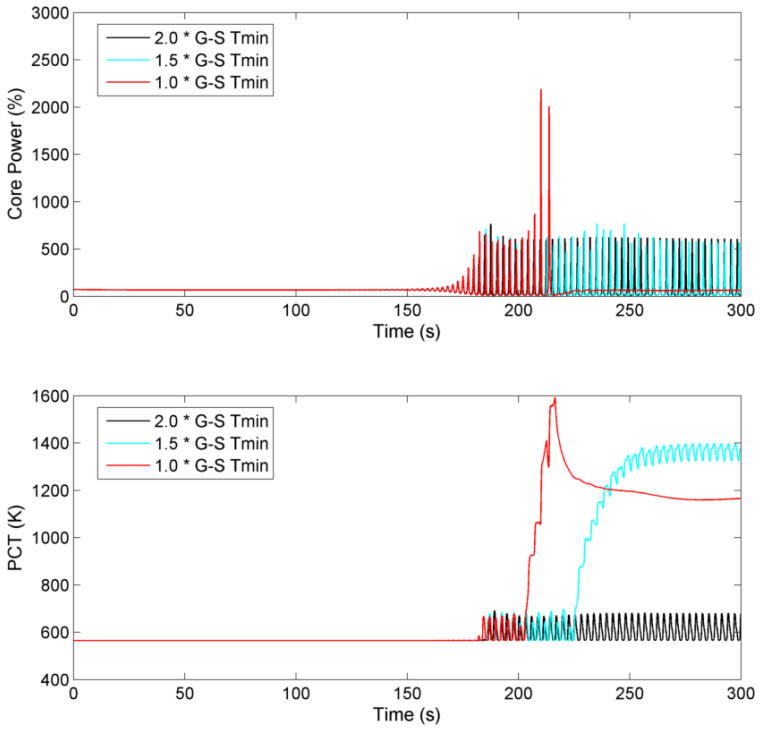

Fig. 9 - Core power (top) and peak clad temperature (PCT) (bottom) during the hypothetical ATWS-I event, using three different multipliers to adjust the internally-calculated T_{min} values

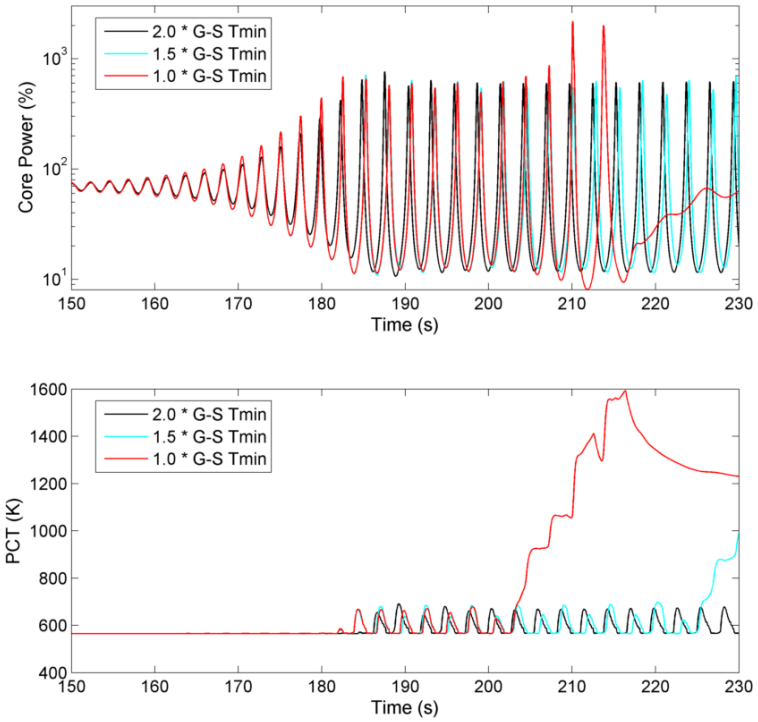

Fig. 10 - Close-up of core power (top) and PCT (bottom) for the T_{min} study

This study has treated modifications to CHF and T_{min} separately, in order to parse out the effects of each term. However, in practice, a highly wettable cladding material may increase *both* the CHF and T_{min} values simultaneously, and vice versa for a material with poor wettability characteristics. Therefore, the same conclusions should still apply: namely, increasing the wettability of a cladding material is expected to have a beneficial effect in terms of delaying or preventing large increases in cladding temperature during postulated ATWS-I events. These calculations have shown that changes in CHF result in changes in time to respond to an ATWS event. In addition, a cladding material with higher CHF may increase the time before clad melting or other severe consequences.

3. REVIEW OF SELECTED RECENT CHF EXPERIMENTS RELEVANT TO ATF CLADDING MATERIALS

The following sub-sections review some selected pool boiling CHF-related experiments in the literature. These experiments are pool boiling experiments at atmospheric pressure for SiC-coated, Cr-coated, and SiC monolith materials. It is notable that none of these experiments have addressed FeCrAl or SiC-SiC composite materials, two of the particularly promising candidates for cladding materials under investigation under the AFC. Pool boiling and flow boiling experiments for these materials are a key need for the eventual deployment of candidate ATF materials.

Pool-boiling CHF is different than flow boiling CHF. There is a significant dependence of flow boiling CHF on the mass flux of the fluid. Several example datasets are shown in Fig. 11. These example datasets are from Reference 20 and are relevant for natural circulation conditions. The data indicate that increasing mass flux yields increasing values of CHF. This particular set of experiments is relevant for light water small modular reactors (SMRs) cooled by natural circulation, where the pressure is high and the mass flux is low to moderate. A similar set of experiments was conducted for research reactors [21] with data collected at low mass flux and low pressure. This is just an illustration of the dependence of

CHF on one parameter, mass flux. Surface wettability is another example of an important parameter, as illustrated in Reference 8. One main focus of the present report is the impact of surface wettability on CHF. Recent efforts in the literature have shown that CHF of ATF cladding concepts in pool boiling can be significantly different than the reference zirconium-based cladding material [22 - 24].

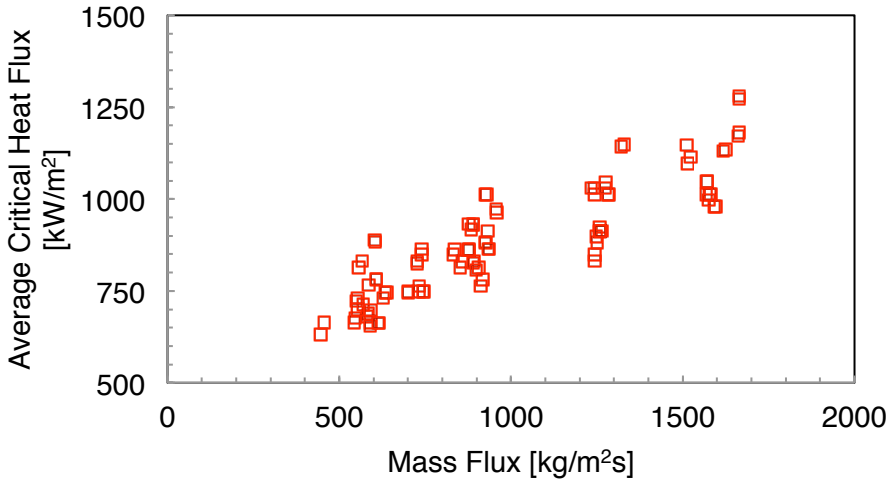

Fig. 11. High pressure CHF data for non-uniform heat fluxes, P < 17 [MPa], and G < 1700 [kg/m^{2}s], data is from Greenwood et al. [20].

3.1 POOL BOILING CHF ON SILICON CARBIDE AND CHROMIUM COATED ZIRCALOY AT ATMOSPHERIC PRESSURE: KAM, D. H., ET AL [22]

One set of recent experiments from the literature includes pool-boiling experiments with SiC- and Cr-coated Zircaloy plates [22]. The SiC-coated plates were produced using physical vapor deposition sputtering and the Cr-coated plates were produced using an electroplating process on the surface of the Zircaloy cladding. The measured surface roughness was similar in all cases. Compared to Zircaloy, SiC-coated Zircaloy plates showed ~40% higher values of pool boiling CHF and Cr-coated Zircaloy plates showed ~25% lower values of CHF. The measured values of pool boiling CHF showed good agreement with the Kandlikar analytical model [7].

The Kandlikar model, described in Reference 7, is intended for prediction of pool-boiling CHF for water, refrigerants, and cryogenic liquids. In formulating this theoretical model, Kandlikar recognized that including contact angle, surface orientation, and subcooling effects are important to accurately model CHF [7]. The model predicts the parametric trends of CHF as a function of dynamic receding contact angle and subcooling [7]. The measured values of CHF from Reference 22 are in good agreement with predictions from Reference 7. The Kandlikar model is:

$$q_c'' = h_{fg}\sqrt{\rho_g}\left(\frac{1+cos\beta}{16}\right)\sqrt[4]{\sigma g(\rho_l-\rho_g)}\sqrt{\frac{2}{\pi}+\frac{\pi}{4}(1+cos\beta)cos\phi} \quad (3)$$

where β is the dynamic receding contact angle and ϕ is the orientation of a bubble on the heater surface.

The pool boiling experiments in Reference 22 indicate that CHF is enhanced with SiC coating and this enhancement increases with increasing thickness of the SiC layer. This is due to the hydrophilic

properties of SiC [22]. CHF was enhanced with SiC even though the surface roughness was similar for all of the plates in the experiment, which included Cr-coated Zircaloy, Zircaloy, and stainless steel plates.

3.2 TRANSIENT POOL BOILING UNDER SATURATION CONDITIONS WITH CHROMIUM COATING AT ATMOSPHERIC PRESSURE: LEE, C.Y., ET AL. [23]

Recent experiments from the literature were focused on a Cr-coated Nb rodlet under rapid cooling (quench) conditions. Cr-coating was applied to the Nb rodlet using a plating method. The experiments indicated that the Cr-coated rodlets featured a significantly longer quenching duration than the rodlets without Cr-coating. The rodlets had a similar surface roughness with and without Cr-coating. This finding (longer quench time) is consistent with the finding in Reference 22, which indicates hydrophobic characteristics of Cr-coating.

3.3 POOL BOILING ON SILICON CARBIDE MONOLITHIC POOL BOILING ON SILICON CARBIDGE MONOLITH MATERIAL AT ATMOSPHERIC PRESSURE: SEO, G. H., ET AL. [24]

Another set of pool boiling experiments in the literature focus on the CHF properties of SiC monolith material [24]. The experiments were conducted via joule heating of SiC and Zr tubes. The experimentally determined CHF of the SiC monolith tube was approximately 60% higher than that of the Zircaloy tube [24]. Additionally, the SiC tube had no visible damage after experiencing the formation of stable film boiling, but the Zircaloy cladding tube exhibited significant damage leading to eventual fragmentation. These results indicate potentially significant enhancement in CHF behavior with SiC tube material. The study observed: *"SiC cladding has the sustainable structural integrity with visual observation after the CHF occurrence and can be advantageous in securing a high safety margin for nuclear power reactor applications."* Additionally, Reference 24 suggests that the thermal properties (e.g. thermal conductivity) of un-irradiated SiC monolith contribute to the increase in CHF.

4. WETTING CHARACTERISTICS OF FeCrAl MATERIAL EXPOSED TO PWR AND BWR RELEVANT TEMPERATURES AND WATER CHEMISTRY

Wetting properties including contact angle are a key parameter that impacts the boiling heat transfer performance for candidate ATF cladding materials. The focus of this section of the report is on some of the wetting characteristics of FeCrAl alloys. Static advancing contact angle measurements were performed at the University of New Mexico (UNM) using an automated contact angle machine following a standard procedure described in Section 4.2.

4.1 EXPERIMENTAL SAMPLES

Oak Ridge National Laboratory (ORNL) provided UNM with a set of representative ATF and baseline cladding material samples including Stainless Steel (310SS), Zirc-4, and different composition of FeCrAl alloys. These samples are "as machined" or exposed to prototypical BWR and PWR conditions tested in 3.78 l (1 gallon) 316 stainless steel (SS) autoclaves. The autoclave tests were performed in a simulated PWR water chemistry, simulated BWR hydrogen water chemistry (HWC), and BWR normal water chemistry (NWC) with details of the environmental conditions provided in Table 2

[25]. The specific samples are also summarized in Table 3. The samples were immersed in autoclave conditions for approximately one year.

Table 2. Summary of autoclave conditions for immersion tests.

Autoclave	**Chemistry**	**Temp. (°C)**	**pH**	**Pressure (MPa)**
PWR	3.57 ppm H_2	330	7.2	15
BWR-HWC	0.3 ppm H_2	290	5.6	7
BWR-NWC	1.0 ppm O_2	290	5.6	7

Table 3. Summary of provided samples.

Sample #	Material	As Machined	PWR	BWR-HWC	BWR-NWC
1	Stainless Steel	X			
2			X		
3	310 SS			X	
4					X
5		X			
6	Zirc-4		X		
7				X	
8					X
9	Fe12Cr5Al (83.6: 12 : 4.4)	X			
10	Fe13Cr4Al (83.0 : 13 : 3.9)	X			
11	Fe12Cr5Al		X		
12	Fe13Cr4Al-SG		X		
14	Fe12Cr5Al			X	
15	Fe13Cr4Al-SG			X	
17	Fe12Cr5Al				X
18	Fe13Cr4Al-SG				X

4.2 SURFACE ROUGHNESS AND STATIC ADVANCING CONTACT ANGLE MEASUREMENT PROCEDURES

A Dektak 150 stylus profiler was used to measure the surface roughness of different samples listed in Table 3. The stylus has 12.5 μm radius using 1 mg force to measure "hill and valley" values. An average of 4 standard scans were performed for each sample double faces. The scan length was 8 mm with 1.33 μm/s scan rate. The collected data from each scan was analyzed using the Dektak software to determine the average roughness, Ra, of each scan. The calculated roughness values for each surface (double faces) were averaged.

The American Society of Testing Materials (ASTM) provides a fully detailed standard procedure for measuring surface wettability by advancing contact angle measurement [26, 27]. The procedure summarizes the necessary steps for obtaining consistent results on contact angle measurement using a liquid droplet on the substrate. The number of droplets, droplet liquid type, volume of the droplet, and measuring time are specified in the ASTM standards. According to the standard, the contact angle can be quantified by averaging the measured angle of three different droplets on the same surface and each has a volume less than 20 μL. The measuring time from the moment of attaching the droplet to the surface

should not exceed 30 seconds to avoid the rapid change of droplet volume either by evaporation or diffusion on the substrate. Deionized water was used for this series of measurements with a droplet volume ranged between 16-20 μL. The contact angle was recorded for 60 times in less than 30 seconds. The contact angle measured for three different droplets on the same metal substrate was averaged to present the contact angle for specific surface. The average contact angle was also used to compare different surface measurements.

4.3 SURFACE ROUGHNESS MEASUREMENT RESULTS

As described in the surface roughness procedure, each sample had between 3 to 6 scans depending on the size and the condition of the sample. Scan routes were selected to cover most of sample's surface and avoid any surface scratches. Fig. 12 shows the three individual scans on Zirc-4-PWR sample. In each scan the average roughness was presented as calculated by the Dektak software. The three scans are collectively presented in Fig. 12d with the overall average roughness value. The same procedure was applied for all other samples and the final average roughness values are presented in Fig. 13.

As shown in Fig. 13, for the same sample material (310SS, Zirc-4, and FeCrAl), the final roughness values experience a slight difference for different testing conditions: as machined, BWR-NWC, BWR-HWC, and PWR. For example, the FeCrAl samples have roughness values of 0.59, 0.61, 0.54, and 0.63 μm for as machined, BWR-NWC, BWR-HWC, and PWR testing condition respectively. These values are within ± 8% from an average roughness value of 0.59 μm. The FeCrAl alloy samples have a higher roughness value compared to Zirc-4 and 310 SS for all types of testing conditions.

As the surface roughness increases, the wetted surface area and/or active nucleation site density also increases and this is typically expected to yield higher CHF.

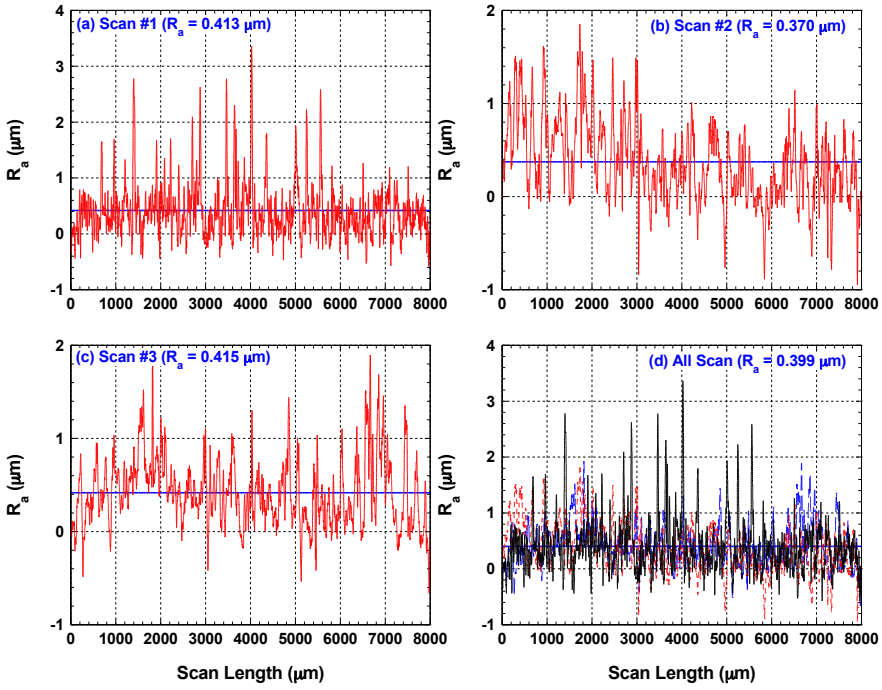

Fig. 12. Individual stylus scan data on Zirc-4-PWR sample (a-c) and collective measurements (d).

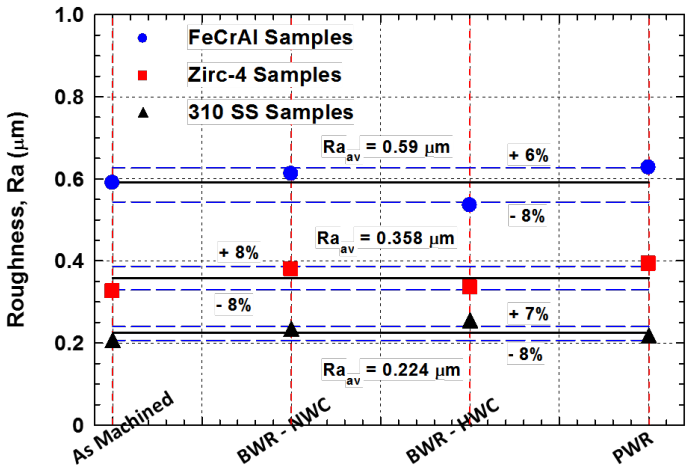

Fig. 13. Measured average surface roughness, Ra for all samples.

4.4 STATIC ADVANCING CONTACT ANGLE MEASUREMENT RESULTS

Before measurement of the contact angle, it was visually observed that the ORNL test samples feature different degrees of oxidation (see Fig. 14). "As machined" samples have no oxidation or at most minor oxidized spots. Samples that were tested in the autoclave under the appropriate chemistry conditions are substantially oxidized and mostly colored black. It is notable that surface oxidation has shown to result in an increase of surface wettability and reduced contact angle [28].

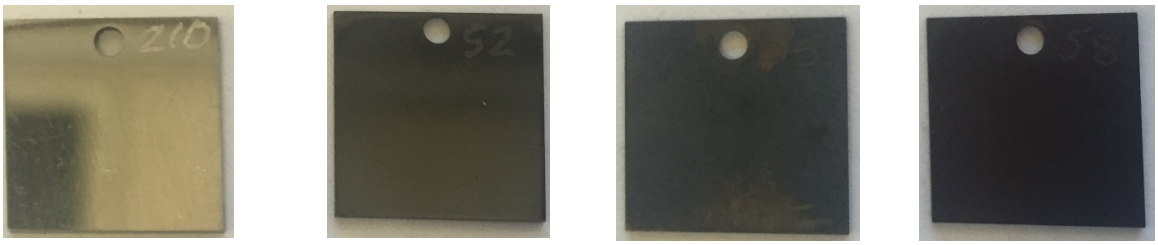

1. "As machined" 2. BWR-HWC 3. PWR-HWC 4. BWR-NWC

Fig. 14. Sample photographs for Fe13Cr4Al-SG tested under different chemistry conditions.

Three different droplets (16-20 µL) were used to measure the contact angle on "as machined" stainless steel (310SS). Measured angles for these droplets for less than 30 seconds are shown in Fig. 15a (open symbols). The measured data was then averaged and presented in the same figure with a solid line. The figure also shows the uncertainty in the measured angle for the three droplets to be within ± 3.5%. The same analysis was carried out for other three 310SS samples examined in the autoclave under PWR-HWR, BWR-HWC and BWR-NWC (see Table 2 and Table 3) and results are presented in Fig. 15b, Fig. 15c, and Fig. 15d. The uncertainties of the measured contact angle of these three samples are less than ±3, ±2%, and ±4.5% respectively.

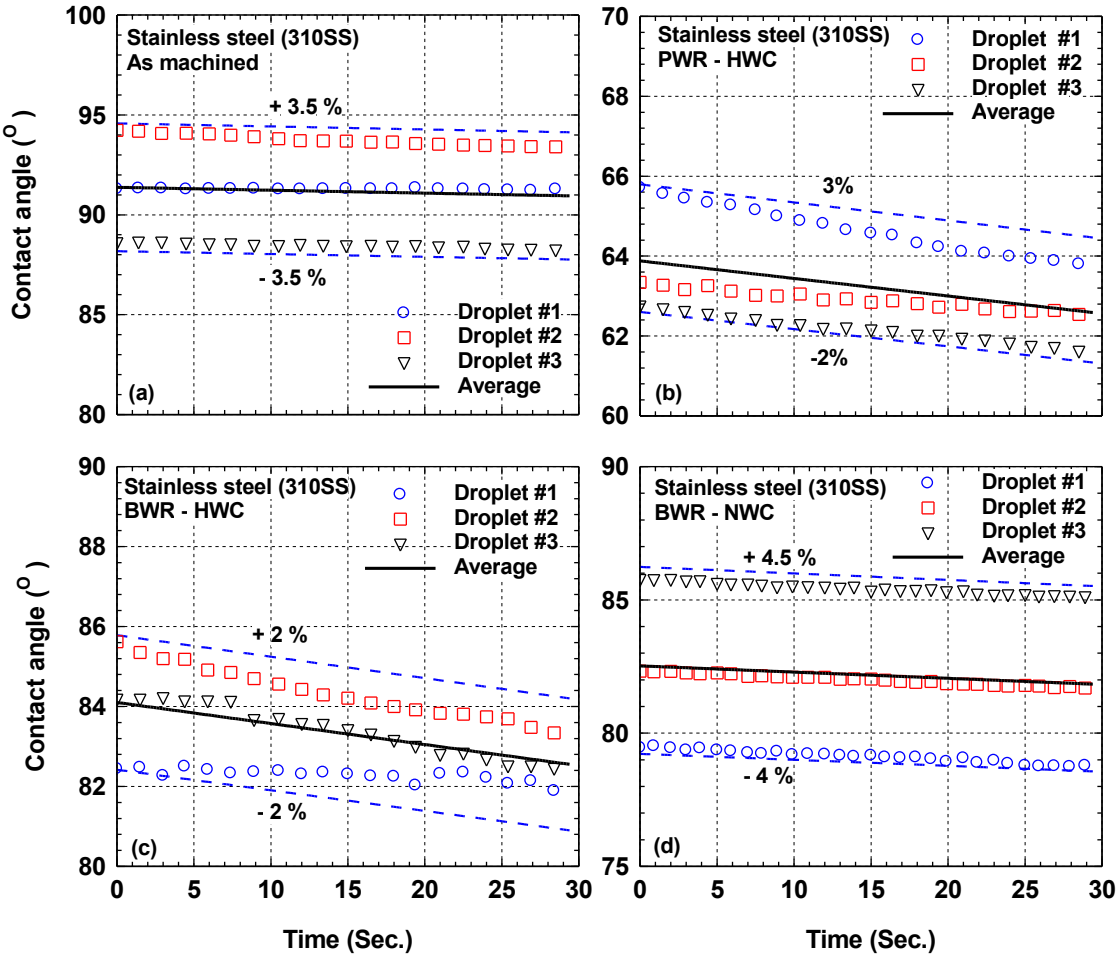

Fig. 15. Measured contact angle for 310SS samples.

A similar approach was applied for all samples listed in Table 3 and results are shown in Fig. 16, Fig. 17, and Fig. 18. The average contact angles determined in Fig. 15 - Fig. 18 are compared in Fig. 15.

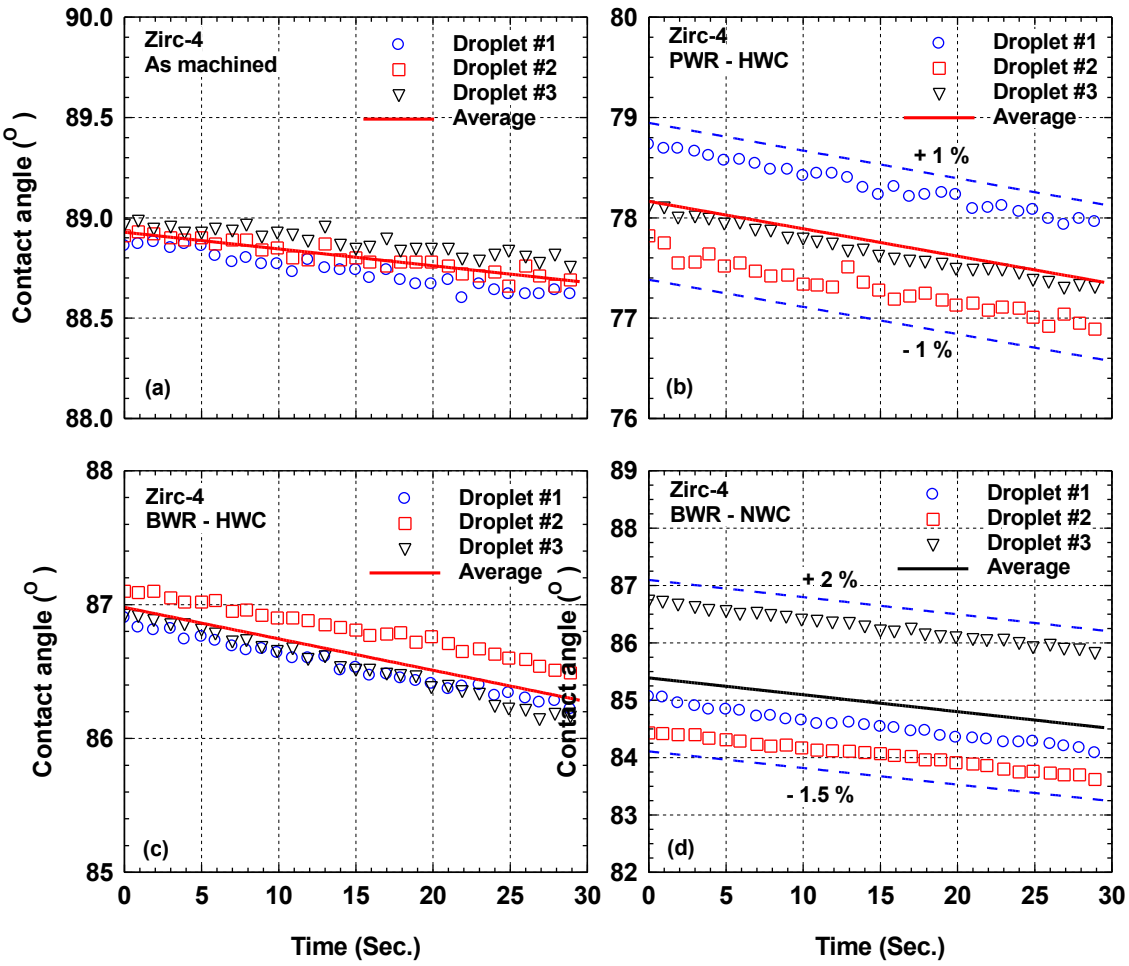

Fig. 16. Measured contact angle for Zirc-4 samples.

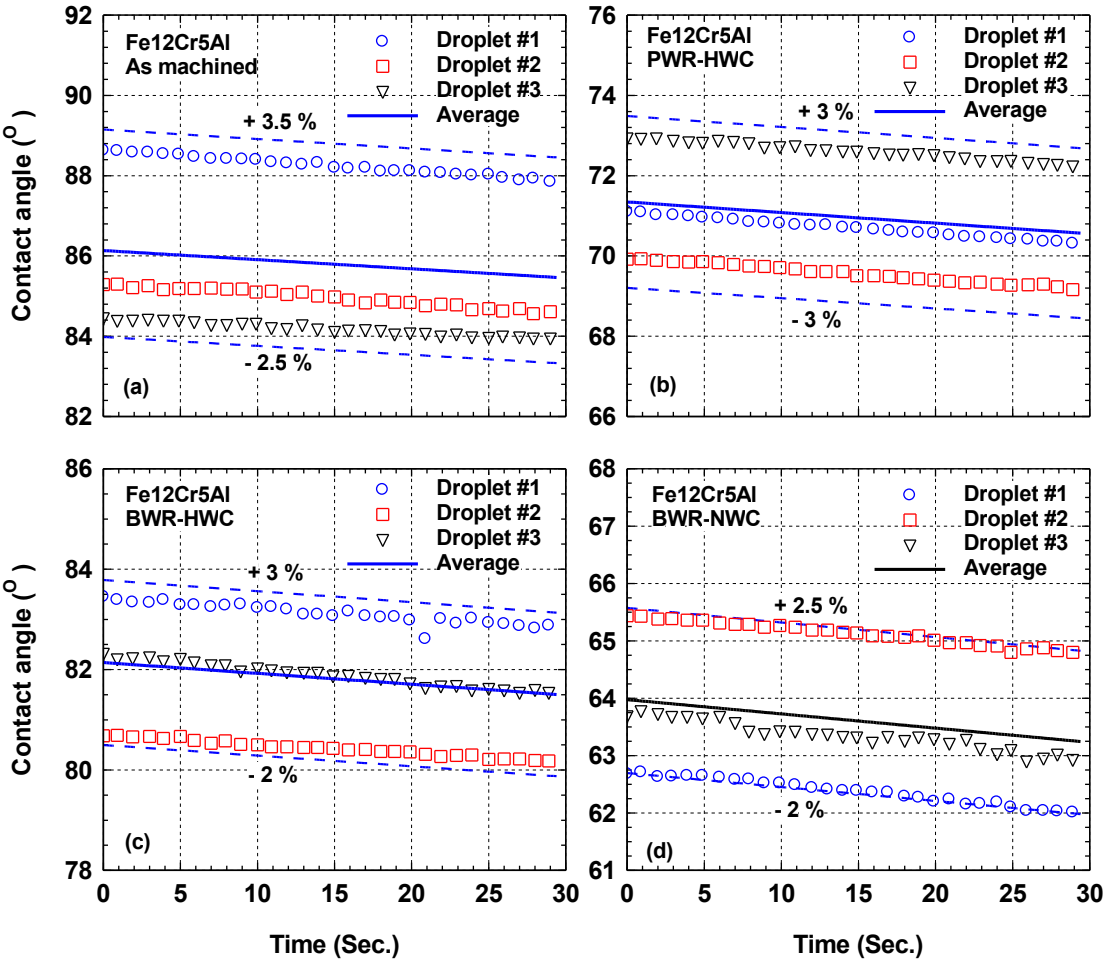

Fig. 17. Measured contact angle for Fe12Cr5Al samples.

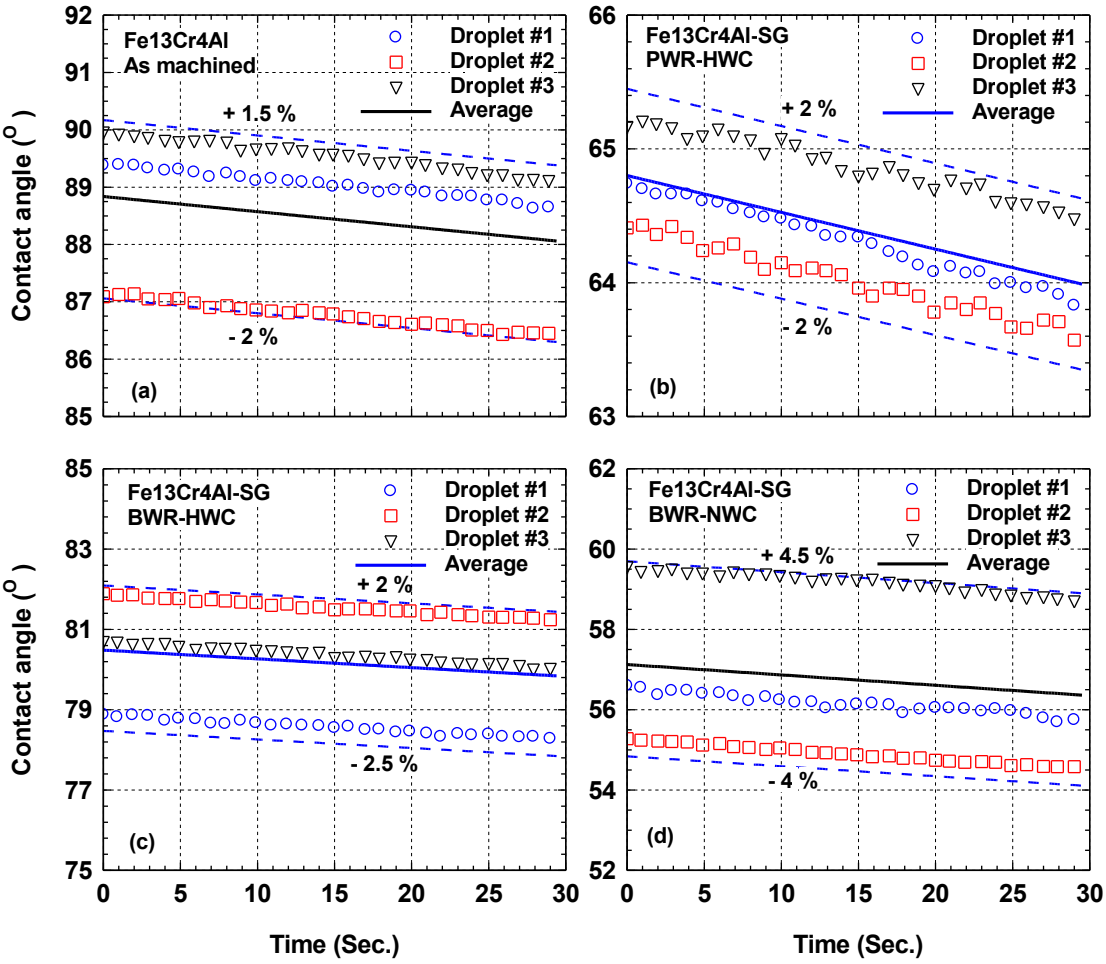

Fig. 18. Measured contact angle for Fe13Cr4Al samples.

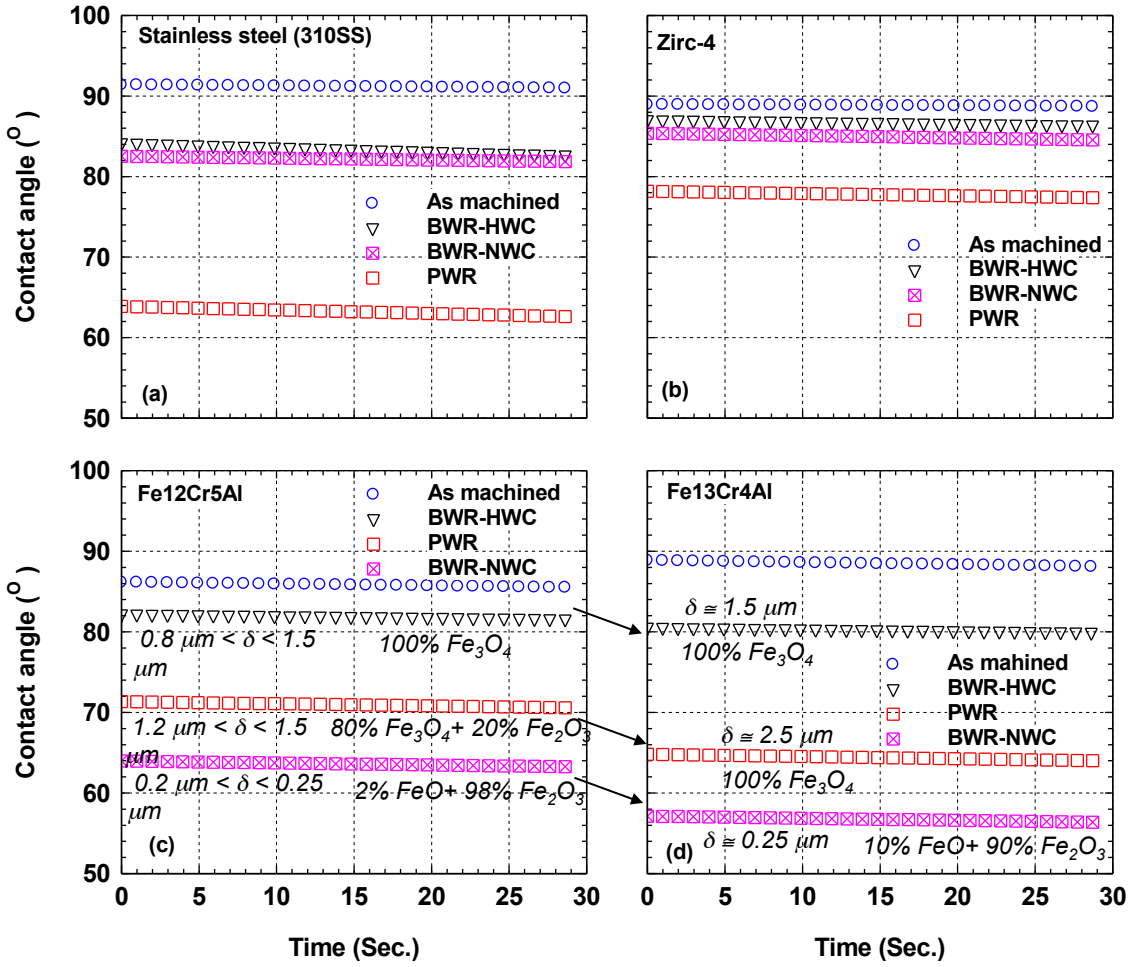

Fig. 19. Comparison of measured contact angle for different samples, with information about oxide layer thickness of the different samples.

The measured advancing contact angles in Fig. 19 show that oxidized surfaces (BWR-HWC, BWR-NWC and PWR-HWC) have lower contact angle compared to the non-oxidized surfaces ("as machined"). Surfaces with a higher degree of oxidation have a lower measured contact angle. For 310SS and Zirc-4 samples (Fig. 19a and Fig. 19b), the contact angle decreased marginally as surface oxidation increased for "as machined", BWR-HWC, BBWR-NWC, and PWR-HWC respectively.

Both FeCrAl alloys (Fig. 19c and Fig. 19d) exhibit consistent behavior with the different water chemistry and their contact angle decreases significantly as surface oxidation increases for as machined, BWR-HWC, PWH-HWC, and BWR-NWC respectively. Based on the contact angle results, FeCrAl alloys (Fe13Cr4Al) are expected to have the highest CHF in both pool and flow boiling experiment under each of the different chemistry conditions (Table 2).

5. SUMMARY

This deliverable is a scoping survey of thermal-fluids evaluation and confirmatory experimental validation requirements of accident tolerant cladding concepts with a focus on boiling heat transfer characteristics. The key takeaway messages of this report include:

1. CHF prediction accuracy is important and the correlations may have significant uncertainty.

2. Surface conditions are important factors for CHF, primarily the wettability that is characterized by contact angle. Smaller contact angle indicates greater wettability, which increases the CHF. Surface roughness also impacts wettability. Results in the literature for pool boiling experiments indicate changes in CHF by up to 60% for several ATF cladding candidates.

3. The measured wettability of FeCrAl (i.e., contact angle and roughness) indicates that CHF should be investigated further through pool boiling and flow boiling experiments.

4. Initial measurements of static advancing contact angle and surface roughness indicate that FeCrAl is expected to have a higher CHF than Zircaloy. The measured contact angle of different FeCrAl alloy samples depends on oxide layer thickness and composition. The static advancing contact angle tends to decrease as the oxide layer thickness increases.

A parametric evaluation of example transients in PWRs and BWRs illustrates the potential impact of changes in CHF on reactor performance and safety characteristics. These transient cases show that changes in CHF can have a significant impact on safety margins as well as transient and accident progression. These example transients illustrate that system analysis codes (e.g. TRACE, RELAP5-3D, RELAP7) need additional data to accurately predict ATF cladding temperatures during some transients.

Recent pool boiling experiments in the literature with SiC and Cr-coated samples indicate that CHF can change by up to 60%. These changes in CHF depend on the wettability, surface roughness, and thermal properties of these materials.

For FeCrAl, the relationship between CHF and the properties of the oxide layer (e.g. thickness, porosity, etc.) is the subject of future work.

6. REFERENCES

1. Carmack, J., K. Barrett, and H. MacLean-Chichester. *Light Water Reactor Accident Tolerant Fuels Irradiation Testing*. No. INL/CON-15-34949. Idaho National Laboratory (INL), Idaho Falls, ID (United States), 2015.

2. Terrani, Kurt A., Steven J. Zinkle, and Lance Lewis Snead. "Advanced oxidation-resistant iron-based alloys for LWR fuel cladding." *Journal of Nuclear Materials* 448.1 (2014): 420-435.

3. Rebak, Raul B., et al. "Resistance of Advanced Steels to Reaction with High Temperature Steam as Accident Tolerant Fuel Cladding Materials." *CORROSION 2014*. NACE International, 2014.

4. Bragg-Sitton, S. “Overview of International Activities in Accident Tolerant Fuel Development for Light Water Reactors,” Idaho National Laboratory, United States April 24, 2014.

5. Snead, M., et al. *Technology Implementation Plan ATF FeCrAl Cladding for LWR Application*. No. ORNL/TM--2014/353. Oak Ridge National Lab.(ORNL), Oak Ridge, TN (United States), 2015.

6. Brown, Nicholas R., Michael Todosow, and Arantxa Cuadra. "Screening of advanced cladding materials and UN–U 3 Si 5 fuel." *Journal of Nuclear Materials* 462 (2015): 26-42.

7. Kandlikar, Satish G. "A theoretical model to predict pool boiling CHF incorporating effects of contact angle and orientation." *Journal of Heat Transfer* 123.6 (2001): 1071-1079.

8. Ahn, Ho Seon, et al. "The effect of liquid spreading due to micro-structures of flow boiling critical heat flux." *International Journal of Multiphase Flow* 43 (2012): 1-12.

9. Desquines, J., et al. "The issue of stress state during mechanical tests to assess cladding performance during a reactivity-initiated accident (RIA)." *Journal of Nuclear Materials* 412.2 (2011): 250-267.

10. Basile, D., and E. Salina. "COBRA-EN an Upgraded Version of the COBRA-3CIMIT Code for Thermal-Hydraulic Transient Analysis of Light Water Reactor Fuel Assemblies and Cores." *Cornpartimento di Milano* (1999).

11. Reddy, D. G., and C. F. Fighetti. "Parametric Study of CHF Data, Volume 2: A Generalized Subchannel CHF Correlation for PWR and BWR Fuel Assemblies." *EPRI report for project RP* 813 (1983).

12. Odar, F. "TRAC/RELAP advanced computational engine (TRACE) V5.0 user manual," U.S. Nuclear Regulatory Commission (2009).

13. Downar, Thomas J., et al. "PARCS: Purdue advanced reactor core simulator." Proc. Int. Conf. on the New Frontiers of Nuclear Technology: Reactor Physics, Safety and High-Performance Computing. 2002.

14. Kozlowski, Tomasz, et al. "TRACE/PARCS VALIDATION FOR BWR STABILITY BASED ONOECD/NEA OSKARSHAMN-2 BENCHMARK." *The 14th International Topical Meeting on Nuclear Reactor Thermalhydraulics, NURETH-14*. 2011.

15. Xu, Yunlin, et al. "Application of TRACE/PARCS to BWR stability analysis." *Annals of Nuclear Energy* 36.3 (2009): 317-323.

16. Wysocki, A., et al. "TRACE/PARCS analysis of out-of-phase power oscillations with a rotating line of symmetry." *Annals of Nuclear Energy* 67 (2014): 59-69.

17. Wang, Dean, et al. "Implementation and assessment of high-resolution numerical methods in TRACE." *Nuclear Engineering and Design* 263 (2013): 327-341.

18. March-Leuba, José, and José M. Rey. "Coupled thermohydraulic-neutronic instabilities in boiling water nuclear reactors: a review of the state of the art." *Nuclear Engineering and Design* 145.1 (1993): 97-111.

19. Cheng, L. Y., et al. "BWR Anticipated Transients Without Scram Leading to Instability." *Transactions of the American Nuclear Society* 109.1 (2013): 983-986.

20. Greenwood, M.S., J. P. Duarte J.P., and M. Corradini. "Comparison of Experimental Critical Heat Flux Data to Prediction Methods for Conditions Prototypical of Light Water Small Modular Reactors." *NURETH-16*, Aug. 30 – Sep. 4, Chicago, IL, USA, 2015.

21. Yang, Jun, et al. "Study of Critical Heat Flux in Natural Convection–Cooled TRIGA Reactors with Single Annulus and Rod Bundle Geometries." *Nuclear Science and Engineering* 180.2 (2015): 141-153.

22. Kam, Dong Hoon, et al. "Critical heat flux for SiC-and Cr-coated plates under atmospheric condition." *Annals of Nuclear Energy* 76 (2015): 335-342.

23. Lee, Chi Young, Wang Kee In, and Yang Hyun Koo. "Transient pool boiling heat transfer during rapid cooling under saturated water condition." *Journal of Nuclear Science and Technology* (2015): 1-9.

24. Seo, Gwang Hyeok, Gyoodong Jeun, and Sung Joong Kim. "Pool boiling heat transfer characteristics of zircaloy and SiC claddings in deionized water at low pressure." *Experimental Thermal and Fluid Science* 64 (2015): 42-53.

25. Terrani, Kurt A., et al. "Hydrothermal corrosion of SiC in LWR coolant environments in the absence of irradiation." *Journal of Nuclear Materials* 465 (2015): 488-498.

26. American Society of Testing Materials (ASTM), Standard Test Method for Surface Wettability and Absorbency of Sheeted Materials Using an Automated Contact Angle, Designation: D 5725 – 99, 2008.

27. American Society of Testing Materials (ASTM), Standard Practice for Surface Wettability of Coatings, Substrates and Pigments by Advancing Contact Angle Measurement, Designation: D7334 – 08, 2013.

28. Hong, Kwang Taek, Harris Imadojemu, and R. L. Webb. "Effects of oxidation and surface roughness on contact angle." *Experimental Thermal and Fluid Science* 8.4 (1994): 279-285.